PHYSICAL REVIEW B VOLUME 14, NUMBER 7 1 OCTOBER 1976

Nuclear magnetic resonance and relaxation in vitreous and liquid B_2O_3 and B_2S_3

Mark Rubinstein
Naval Research Laboratory, Washington, D. C. 20375
(Received 10 May 1976)

The vitreous and liquid phases of B_2O_3 and B_2S_3 are investigated by the techniques of continuous-wave and pulsed nuclear magnetic resonance. The temperature dependence of the ^{11}B line shape and spin-lattice relaxation rate are studied up to 650°C for B_2O_3 and 250°C for B_2S_3. A structural model involving the progressive fragmentation with increasing temperature of the linked network structure, which exists at ambient temperatures, is advocated for both glasses.

INTRODUCTION

The vitreous and the liquid state of glass formers are closely related. Both states of matter are, by definition, characterized by the absence of long-range order. Many glasses are formed by cooling from the normal liquid state in such a way that no discontinuous changes occur. Such materials are rigid below the glass transition temperature without the onset of crystallization; these glasses may be defined as supercooled liquids.

Boron oxide (B_2O_3) and boron sulfide (B_2S_3) are two such glasses that can be formed by cooling from the melt. The molten phase of B_2O_3 has been extensively studied by several diverse techniques. This paper reports on the ^{11}B nuclear magnetic resonance and relaxation in the molten and vitreous phases of B_2O_3 and B_2S_3. The structure and dynamics of these materials, as elucidated by NMR techniques, are followed from the room-temperature vitreous phase to the liquid phase at elevated temperatures. This paper is complementary to a previous publication in which the temperature dependence of the ^{11}B NMR in B_2O_3 was investigated from -100 to $+200$ °C.[1]

In the present publication these measurements are extended to higher temperatures, and the transition from the vitreous to the molten state is investigated in B_2O_3. Similar measurements in the related glass, B_2S_3, are also reported. In the liquid phase the system dynamics are governed by self-diffusion. The self-diffusion process is characterized by a broad distribution of correlation times, which begins to narrow at the highest temperatures. In the vitreous state, the nuclear spin-lattice relaxation is determined by low-frequency vibrations and two-level "defects" which are characteristic of glasses in general.

B_2O_3 BACKGROUND

Of all the simple glasses, boron oxide has probably received the most careful attention from physicists. Mozzi and Warren[2] have investigated the structure of vitreous B_2O_3 by x-ray diffraction, and found that this glass is best modeled by a random network of six-membered B_3O_6 boroxol rings which are linked by a sharing of corner oxygens, and with randomness in orientations about the B-O bond directions at these corner oxygens. Ambient temperature NMR line-shape studies[3] of B_2O_3 reveal that each boron atom in the glass is coordinated with three oxygen atoms and resides in a site of nearly trigonal symmetry. The Raman spectrum of vitreous B_2O_3 exhibits a strong Raman-active line at 808 cm^{-1} which has been associated with the symmetric breathing mode of the boroxol rings.[4–6] Young and Westerdahl found that the intensity of the 808-cm^{-1} line is strongly temperature dependent in the molten phase, and disappears over 800 °C. This observation provides evidence that a structural change occurs in liquid boric oxide between 400 and 1400 °C which involves a gradual reduction in the number of boroxol rings as a function of increasing temperature.

Viscosity measurements[7–9] on B_2O_3 show non-Arrhenius behavior in the region from 300 to 800 °C; above 800 °C a constant activation energy is found. Sperry and Mackenzie interpret this as further evidence of temperature-dependent structure, and deduce that the structure of molten B_2O_3 above 800 °C is that of a liquid composed of small un-ionized molecules. These molecules are presumably the same as those which exist in the vapor phase of B_2O_3.

The Catholic University–National Bureau of Standards group has greatly contributed to our understanding of vitreous and molten B_2O_3. Beginning in 1965, in a series of papers, this group has conducted an extensive investigation on the viscous relaxation and non-Arrhenius behavior in B_2O_3, performing ultrasonic relaxation[10] density[11] and viscosity[7] measurements. These workers have demonstrated the existence of a wide distribution of activation energies in the melt, and quantified this distribution. These measurements were later extended to lower temperatures by Bucaro, Dardy,

and Corsaro[12] using light-scattering correlation and pressure-jump volume relaxation techniques.

Thanks to Krogh-Moe[13] and Mackenzie[14] a model of the temperature-dependent structure of B_2O_3 has emerged. A variant of their ideas is shown in Fig. 1, where the assumed structural variation with temperature is sketched. In the vitreous phase, boron trioxide is a random linked network of BO_3 groups, containing a predominant number of six-membered boroxol rings. In this phase, each boron atom resides near the center of a planar triangle determined by its three bonding oxygens. This configuration remains stable until the glass transition temperature $T_g = 280$ °C is reached. Above T_g, an increasing number of bonds begin to snap off resulting in a structure composed of disassociated units of various sizes. These fragments, which are composed primarily of boroxol rings, can slip past each other, allowing viscous flow to occur. As the temperature is raised the area of fragments decrease, and the number of six-membered rings is reduced accordingly. Above 800 °C, the structure has completely disassociated into a fluid of B_2O_3 molecules. These molecules are assumed to be identical to those present in the vapor phase of B_2O_3, and which have been identified from spectroscopic data[15] as existing in a bipyramidal structure. The broad distribution of activation energies observed in the intermediate phase of B_2O_3 is correlated with the distribution of fragment sizes.

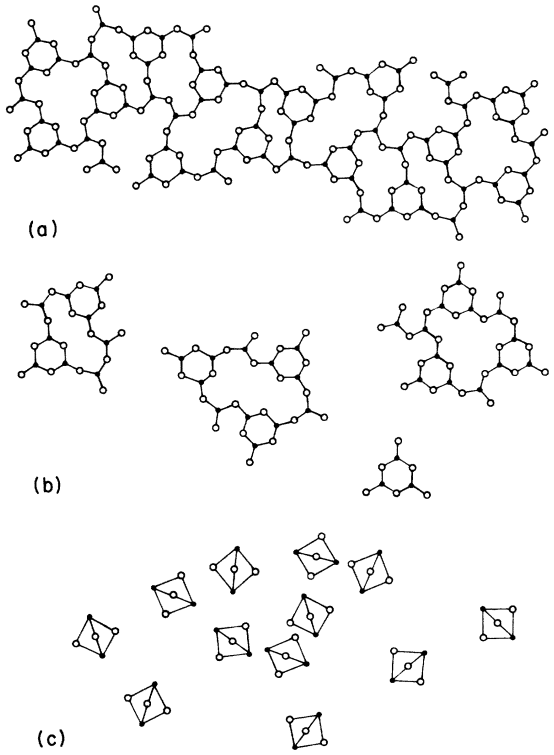

FIG. 1. Schematic representation of proposed structural variation of B_2O_3 with temperature. Temperature increases from (a) to (b) to (c). Filled circles represent boron (after Ref. 14).

B_2S_3 BACKGROUND

Although a considerable amount is known about the physical properties of B_2O_3, very little is known concerning B_2S_3. The infrared and visible spectra of gaseous B_2S_3 has been examined at high temperatures.[16] From this study, the B_2S_3 molecule is thought to have a twisted zigzag structure in the vapor phase. No data on viscosity, density, Raman spectra, etc., exist for B_2S_3. Recently, Hendrickson and Bishop[17] have investigated glassy B_2S_3 by continuous-wave NMR. These authors observe a quadrupolar broadened spectrum at room temperature which is nearly identical to the quadrupolar broadened spectrum of B_2O_3. The width of the broad ^{11}B line was temperature independent; however, with increasing temperature the broad line gradually vanished, and a narrower line grew in its place. The authors attribute this phenomenon to a structural change which involves conversion of boron from three to four coordination, as occurs in borate glasses with the addition of alkali oxide. Above 100 °C this narrow line gradually disappeared, and an extremely narrow line grew in its place with increasing temperature. Hendrickson and Bishop attribute this change to a motional narrowing process, Resing's "apparent phase change."[18]

The temperature-dependent structure of B_2S_3, as envisioned by Hendrickson and Bishop, is entirely different from that of B_2O_3. An attempt to understand and reconcile these differences provided the motivation for investigating B_2S_3 by pulsed NMR techniques.

INSTRUMENTATION AND SAMPLE PREPARATION

This paper is concerned with temperature variation of the ^{11}B NMR line shape, spin-lattice relaxation time, and transverse relaxation time in the vitreous and molten phases of B_2O_3 and B_2S_3. Continuous-wave NMR spectra were obtained using a Varian V-4200B spectrometer with a boron-free NMR probe. The absorption-derivative spectra were recorded on a Nicolet model 1074 instrument computer, and the line shapes were obtained by using the Nicolet's numerical-integration feature. Pulsed NMR measurements were obtained using a Bruker SXP spectrometer with a specially constructed high-temperature boron-free probe head. Line shapes were obtained by integrating the coherently detected NMR signal with a boxcar aver-

ager,[19] and relaxation times were measured in the conventional manner.[20] All measurements were taken at a frequency of 15.450 MHz, corresponding to a resonance field of 11.31 kOe for the free boron nuclear spin.

Boron-oxide samples, obtained from BD Chemicals, were specified 99.995% pure. Boron-sulfide samples, obtained from ROC/RIC Corp., were nominally 99+% pure. Cylindrical B_2O_3 samples were obtained by melting boron-oxide lumps in a platinum crucible at 1000 °C and pouring the melt into a graphite mold. Cylinders of B_2S_3 glass were made by sealing the B_2S_3 powder in an evacuated sealed quartz tube and heating to 300 °C in an upright position.

RESONANCE AND RELAXATION IN B_2O_3

Elemental boron contains two isotopes: ^{10}B which is 19% naturally abundant and has a nuclear spin $I=3$, and ^{11}B which is 81% abundant with nuclear spin $I=\frac{3}{2}$. This paper is concerned only with ^{11}B which has a sizable nuclear quadrupole moment eQ.[21] In vitreous B_2O_3 the boron nucleus resides in a site of low symmetry where it experiences an electric field gradient eq caused primarily by the electrons which covalently bond the boron atom to the three neighboring oxygen atoms. The strength of the average quadrupole coupling constant in B_2O_3 is $e^2qQ/h=2.66$ MHz.[22]

The effect of the quadrupolar interaction is to shift the NMR frequency from the Larmor precession frequency in the applied magnetic field $\nu_L=\gamma H_0$ by an amount which depends on the quadrupole coupling constant and the angle between the magnetic field and electric-field-gradient axis.[20] In a glass, or a polycrystalline powder, these angles are randomly distributed, and the resulting line shape is a powder pattern average. The central $-\frac{1}{2}\longleftrightarrow+\frac{1}{2}$ transition is broadened by the quadrupole interaction only in second-order perturbation, and hence is considerably narrower than the sidebands. This transition, which is the only one considered in this paper, has a line shape containing two peaks and a discontinuity.[23] The theoretical line shape, assuming a negligible asymmetry parameter, is shown in Fig. 2, together with the observed line shapes in vitreous and polycrystalline B_2O_3.[1] The differences between the amorphous and crystalline line shapes are real, and are caused by the distribution of quadrupole coupling constants in the glass, and by the somewhat different values of the asymmetry parameters in the two materials.

In the molten state, the anisotropic powder pattern will sharpen into a narrow symmetric line, owing to the random motion of the boron nuclei.

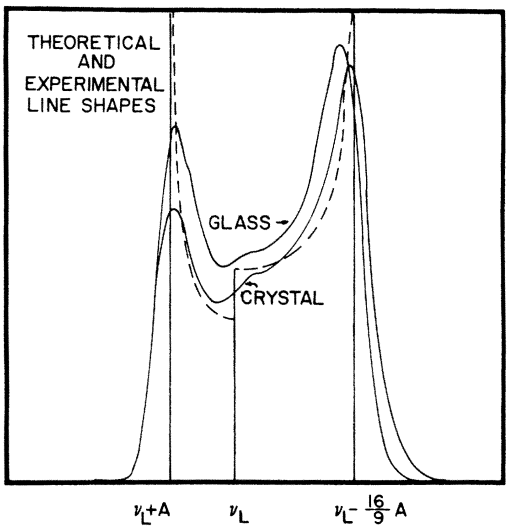

FIG. 2. Resonance line shapes of the central $+\frac{1}{2}\longleftrightarrow-\frac{1}{2}$ transition in vitreous and polycrystalline B_2O_3. The dashed lines are the theoretical powder-pattern line shape of ^{11}B, broadened in second order by an axially symmetric quadrupole interaction, excluding the effects of dipolar broadening $\nu_L=\gamma H_0/2\pi$ and $A=3e^2qQ/64h\nu_L$.

The effects of these thermal motions, which include rotational tumbling and relative translational motion of molecules, or groups of molecules, are responsible for the nuclear spin-lattice relaxation time and the residual quadrupolar linewidth.

In Fig. 3, the temperature dependence of the ^{11}B B_2O_3 line shape is shown. The rigid-lattice line shape of Fig. 2 is observed for all temperatures below ~350 °C. Above this temperature the line abruptly vanishes, and no resolvable signal can be observed until 500 °C. A narrow, symmetric resonance line emerges above 500 °C, which then broadens with increasing temperature. The highest temperature attained in these experiments was ~700 °C. The disappearance of the resonance line between 350 and 500 °C is caused by motional broadening effects, which precede the high-temperature motionally narrowed region.

A more detailed description of this process necessitates an investigation of the temperature dependence of the spin-lattice relaxation time T_1. The spin-lattice relaxation in the vitreous phase of B_2O_3 has been studied previously; Szeftel and Alloul[24] investigated the temperature dependence of T_1 in the low-temperature range from 1.2 to 77 K, and Rubinstein *et al.*[1] investigated the intermediate temperature region 100–500 K (−173 to +200 °C). Both sets of authors observe that the relaxation rate in the glass is much greater than that measured in the polycrystal and is nearly field independent. At low temperatures the relaxation rate varies with temperature as

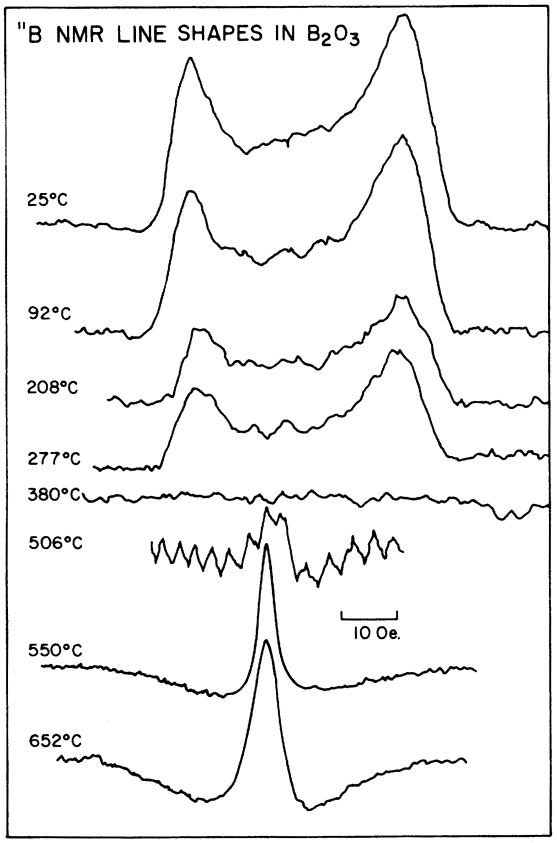

FIG. 3. Temperature variation of the ^{11}B line shape in B_2O_3. Data are obtained at 15.450 MHz.

$$T_1^{-1} = AT^{1.3} , \quad (1)$$

where A is a constant. Around room temperature a T_1 minimum is observed in the temperature dependence, and an increase in T_1 with increasing temperature thereafter.

The almost linear dependence of the relaxation rate on temperature, observed at low temperatures, is believed to be caused by the influence of two-level defects,[25] intrinsic to the amorphous state, on the quadrupolar relaxation.[1,24,26] The T_1 minimum is thought to result from low-frequency lattice vibrations whose lifetimes become extremely short near 300 K. The theoretical expression for this process, which reduces to the usual Van Kranendonk[27] two-phonon Raman process at low temperatures is

$$T_1^{-1} = BT^2\{2\tan^{-1}(\epsilon\tau) - (1/\epsilon\tau)\ln[1+(\epsilon\tau)^2]\} . \quad (2)$$

In Eq. (2), ϵ is the bandwidth of the low-frequency vibrations, $\tau = \tau_0 e^{E/kT}$ is the thermally activated lifetime of these low-frequency vibrations with activation energy E, and B is a constant which is determined by a fit to the experimental data. The band of low-frequency vibrations is assumed to be composed of the "extra" low-lying phononlike excitation which have been found in amorphous materials by specific-heat and Raman studies.[28] The absence of a strong dependence of the magnitude of T_1 on the Larmor frequency below the 300-K T_1 minimum shows that the usual BPP (Bloembergen, Purcell, and Pound) theory[29] or its variants, are not applicable to describe this situation.

It is to be expected, however, that as the temperature is raised to higher values, and self-diffusion becomes thermally activated, an additional T_1 minimum which does obey the BPP equations will be found. This process is also responsible for the motional narrowing of the inhomogeneously broadened linewidth.

Figure 4 displays the temperature dependence of the ^{11}B B_2O_3 spin-lattice relaxation time T_1 from 1 to 1000 K (−272 to +700 °C). The low-temperature data ($-220 \leq T \leq -272$ °C) are that of Szeftel and Alloul. The data in the intermediate temperature range ($-150 < T < 200$ °C) are that of Rubinstein *et al.* The data for $T > 200$ °C are new.

The three disjointed curves in Fig. 4 represent, respectively, Eq. (1) which is applicable at low temperatures, Eq. (2) which is applicable at intermediate temperatures, and Eq. (5), discussed below, which is an appropriate modification of the BPP theory applicable to B_2O_3 in the high-temperature regime.

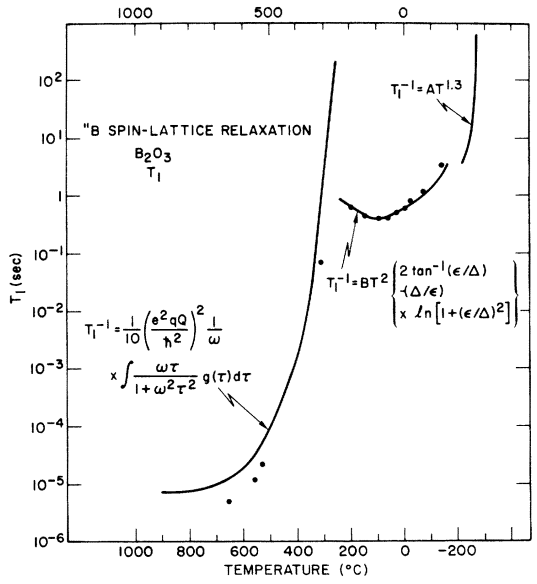

FIG. 4. Temperature variation of ^{11}B spin-lattice relaxation time T_1 in B_2O_3 at 15.450 MHz. Data points are black dots. Curve labeled $T_1^{-1} = AT^{1.3}$ represents data of Ref. 24. The other two disjointed curves show the temperature dependence of the two-phonon contribution and the self-diffusion contribution, respectively.

The spin-lattice relaxation for a nucleus having $I>\frac{1}{2}$ within a molecule which is free to rotate and tumble has been discussed by several authors. These discussions are not entirely consistent, and the correct result is contained in a publication by Hubbard.[30] Hubbard demonstrates that, in general, the relaxation produced by quadrupole interactions is the sum of $I+\frac{1}{2}$ decaying exponential terms if I is half an odd integer. For the particular case $I=\frac{3}{2}$, the dominant relaxation rate is given by the expression

$$\frac{1}{T_1}=\frac{1}{10}\left(\frac{e^2qQ}{\hbar}\right)^2\frac{\tau}{1+\omega^2\tau^2}\,. \tag{3}$$

In Eq. (3) ω is the Larmor frequency expressed in rad/sec and τ is the thermally activated correlation time, for which a unique activation energy can be defined when dealing with a low-viscosity liquid or a gas. For highly viscous materials, it is necessary to describe the correlation time in terms of a distribution of activation energies.

It is an extremely fortunate circumstance that the temperature dependence and the spectral distribution of the activation energies are already known for viscous B_2O_3. The spectrum of relaxation times has been deduced by Tauke, Litovitz, and Macedo[10] from ultrasonic attenuation measurements in the temperature range between 550 and 1000 °C. These authors analyzed their data assuming a log Gaussian distribution function for the distribution of correlation times $g(\tau)$,

$$g(\tau)=(b/\sqrt{\pi})\exp[-b^2\ln^2(\tau/\tau_0)]\,, \tag{4}$$

which is a distribution symmetric in the logarithm of τ centered at τ_0; b is a measure of the width of the distribution. (For a single exponential relaxation process $b=\infty$.) Values of b and τ_0 for B_2O_3 are tabulated in Ref. 10 for nine temperatures between 550 and 1000 °C; for example, at 700 °C $b=0.60$ and $\tau_0=3.18\times10^{-8}$ sec for the relaxational longitudinal modulus, which represents a broad distribution of relaxation times at this temperature. At higher temperatures, the distribution function width decreases; and at temperatures exceeding 900 °C a single relaxation time is indicated. This behavior is in accord with the structural model represented by Fig. 1.

Equation (3) has the obvious generalization for the case of a distribution of correlation times

$$\frac{1}{T_1}=\frac{1}{10}\left(\frac{e^2qQ}{\hbar}\right)^2\frac{1}{\omega}\int_{-\infty}^{\infty}\frac{\omega\tau}{1+\omega^2\tau^2}g(\tau)\,d\tau\,. \tag{5}$$

Values for the integral of Eq. (5), using the lognormal distribution function, have been tabulated by Nowick and Berry[31]; thus the theoretical value for the ^{11}B spin-lattice relaxation time may be calculated at any temperature for which the two parameters τ_0 and b have been measured.

Below 550 °C, the correlation times become too long to be evaluated by ultrasonic attenuation measurements. However, by performing light-scattering correlation measurements and pressure-jump volume relaxation studies in B_2O_3, Bucaro, Dardy, and Corsaro[12] were able to extend the measurement of the correlation time distribution function to temperatures as low as 250 °C. These measurements, together with the ultrasonic results, cover a temperature region for B_2O_3 in which the structural correlation time changes by more than 13 orders of magnitude. Figure 5, taken directly from Ref. 12, displays the temperature dependence of the average correlation time and shows the non-Arrhenius behavior which exists in B_2O_3.

Bucaro *et al.* fit their data to a correlation function $\varphi(t)$ which decays in a fractional exponential fashion

$$\varphi(t)=\exp[(-t/\tau_0)^{\beta}] \tag{6}$$

$\varphi(t)$ is the strain decay function, and its relationship with $g(\tau)$ is discussed by Moynihan *et al.*[32] Like the lognormal distribution, this is a two-parameter fit to the data involving the average correlation time τ_0 and the fractional exponent β. Typical values, e.g., at 310 °C, are $\tau_0=4.4$ sec and $\beta=0.60$. Using the correlation function of Eq. (6) the expression for the ^{11}B spin-lattice relaxation rate becomes

$$T_1^{-1}=\frac{1}{10}\left(\frac{e^2qQ}{\hbar}\right)^2\int_0^{+\infty}\cos\omega t\exp[(-t/\tau_0)^{\beta}]\,dt\,. \tag{7}$$

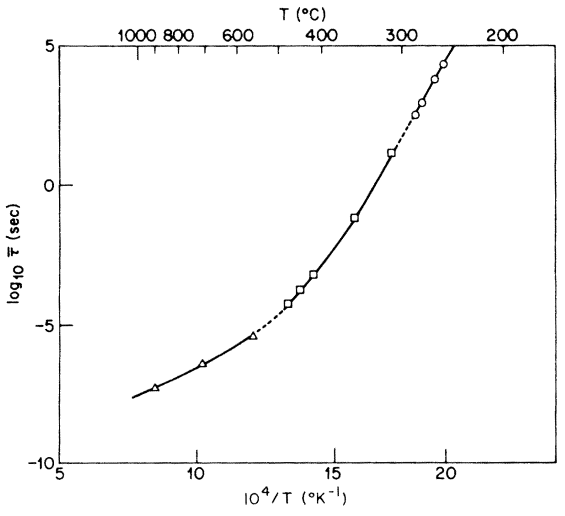

FIG. 5. Temperature dependence of the average correlation times in B_2O_3 from various techniques. Triangles are obtained from ultrasonic measurements, squares from optical correlation measurements, and circles from pressure jump relaxation measurements (from Ref. 12).

Numerical tabulations of the integral in Eq. (7) exist for moderate values of the parameter $(\omega\tau_0)$.[32] For $\omega\tau_0 \gg 1$, which occurs for temperatures below 300 °C, we may use the asymptotic expression

$$T_1^{-1} = \frac{1}{10}\left(\frac{e^2qQ}{\hbar}\right)^2 \frac{1}{\omega}\frac{\beta}{(\omega\tau_0)^\beta} \quad \text{(valid for } \omega\tau_0 \gg 1\text{)} . \qquad (8)$$

Using $e^2qQ/h = 2.66$ MHz and the Larmor frequency $\omega = 97.1 \times 10^6$ rad/sec, together with the data of Refs. 12 and 10, the spin-lattice relaxation time may be calculated as a function of temperature using Eq. (5) above 550 °C or Eq. (7) below 550 °C. We obtain the theoretical curve which is plotted in Fig. 4 in the temperature region between 300 and 900 °C. The measured relaxation time deviates strongly from the theory at low temperatures because the two-phonon Raman process of Eq. (2) is the dominant relaxation process. The small deviations at high temperatures are due to the limitations of the theory: the assumption that the quadrupole coupling constant is temperature independent, and the assumption that the strain correlation time is identical to the correlation time for quadrupolar relaxation. Considering that there are no adjustable constants in the theory, however, the agreement with experiment is good enough to maintain that the high-temperature nuclear relaxation is well understood in terms of the dynamics of the B_2O_3 melt.

RESONANCE AND RELAXATION IN B_2S_3

At room temperature, the ^{11}B line shape in amorphous B_2S_3 closely resembles the room-temperature line shape in B_2O_3, viz., a quadrupole broadened powder pattern characterized by a small asymmetry parameter. Moreover, the quadrupole coupling constant in B_2S_3 $e^2qQ/h = 2.51$ MHz is close in magnitude to the quadrupole coupling constant in B_2O_3, where $e^2qQ/h = 2.66$ MHz. This suggests that the structure of the low-temperature state of boron-sulfide glass is similar to B_2O_3 glass.

As the temperature is raised, a narrow symmetric line appears in the spectrum, and grows at the expense of the powder pattern. The temperature evolution of the line shape is shown in Fig. 6. These line shapes were obtained with a continuous-wave NMR spectrometer by numerically integrating the absorption derivative signal, and are subject to a small distortion caused by the finite amplitude of the modulating magnetic field. Hendrickson and Bishop[17] attributed this line-shape change to a temperature induced conversion of boron from three to four coordination. We will present evidence from nuclear relaxation measurements which indicates, instead, that B_2S_3 glass begins to flow at low temperatures, and the symmetric line is due to the molten component of the sample which gives rise to a motionally narrowed ^{11}B line shape.

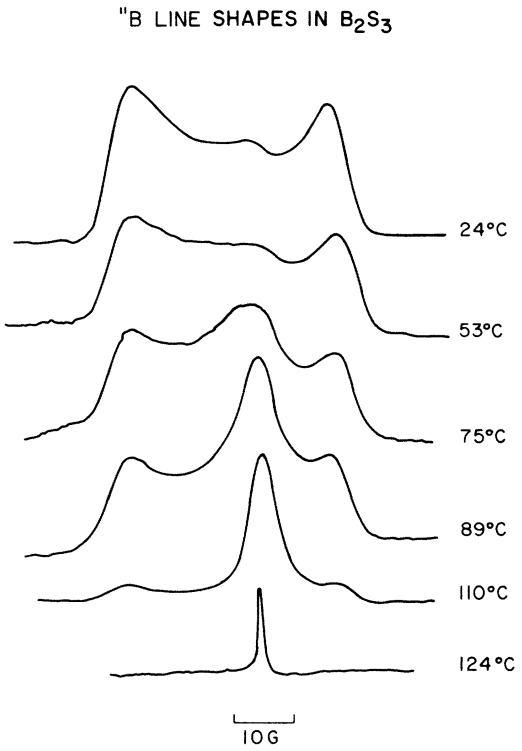

FIG. 6. Temperature variation of the ^{11}B line shape in B_2S_3. Data are obtained at 15.450 MHz.

At temperatures above 100 °C, the modulation amplitude was decreased by an order of magnitude. A weak, but very narrow line (linewidth 0.2 G) can be observed, which grows in magnitude with increasing temperature in the temperature range $100 < T < 200$ °C, and saturates for $T > 200$ °C. The sharp line at the bottom of Fig. 6 was observed under these conditions. This effect was attributed by Hendrickson and Bishop to the onset of motional narrowing. As stated above, however, the line is already motionally narrowed at 100 °C.

The temperature dependence of the ^{11}B spin-lattice relaxation time T_1 in B_2S_3 is shown in Fig. 7. Data points are recorded in the temperature range from 25 to 250 °C. Temperatures higher than 300 °C were difficult to achieve because of the sample's tendency to sublime. The resulting explosion of the quartz container and the consequent evolution of H_2S gas were not found to noticeably enhance the author's popularity with his coworkers.

There exists a difference of two to three orders of magnitude between the relaxation times associated with the low-temperature phase powder-pattern line and the high-temperature phase-sym-

metric line. In the temperature region $80 < T < 100$ °C, where these two resonance shapes coexist, this large difference between their respective T_1's is found to persist. This large difference in relaxation times at identical temperatures is *not* compatible with the hypothesis of Hendrickson and Bishop that the low-temperature phase is a threefold coordinated solid and the higher-temperature phase is a fourfold coordinated solid. Provided the Debye temperature is not altered by the purported change in coordination, the quadrupolar relaxation of three-coordinated and four-coordinated solids are expected to be quite similar.[27] Although four-coordinated or cubic solids have small or zero electric field gradients eq at nuclear sites, which result in small quadrupolar broadening, the spin-lattice relaxation is proportional to the second spatial derivative of the field gradient $\partial^2(eq)/\partial x^2$. This quantity, or its appropriate symmetrized analog, is of the same magnitude in cubic or noncubic crystals. We conclude that the symmetric line is associated with the liquid phase and the powder pattern with the solid phase.

The enhanced relaxation rate, which accompanies the transition depicted in Fig. 6, is caused by the onset of viscous flow; with rising temperature, the bonded solid network breaks up into smaller segments which are increasingly mobile. Such thermally induced motions in the viscous state give rise to spin-lattice relaxation processes described by Eq. (5).

Another argument which supports associating the symmetric line with the liquid, is the absence of inhomogeneous broadening in the symmetric line of B_2S_3. The low-temperature glass phase of B_2S_3 is characterized by inhomogeneous electric field gradients due to random bonding angles and the presence of internal strains. These inhomogeneous fields cause the free-induction decay signal following a single rf pulse to dephase and quickly decay. However, the signal can be regained by the subsequent application of a second pulse: the spin-echo effect. In the liquid state, in the presence of a homogeneous external field, only the free-induction decay is observed; all inhomogeneities have been motionally averaged away. The symmetric line of B_2S_3 does not give rise to a spin-echo signal using a two-pulse sequence, indicating that this line is associated with the viscous phase. The B_2S_3 powder-pattern line, on the other hand, produces a strong spin-echo signal, indicating that this line is associated with the vitreous phase of B_2S_3.

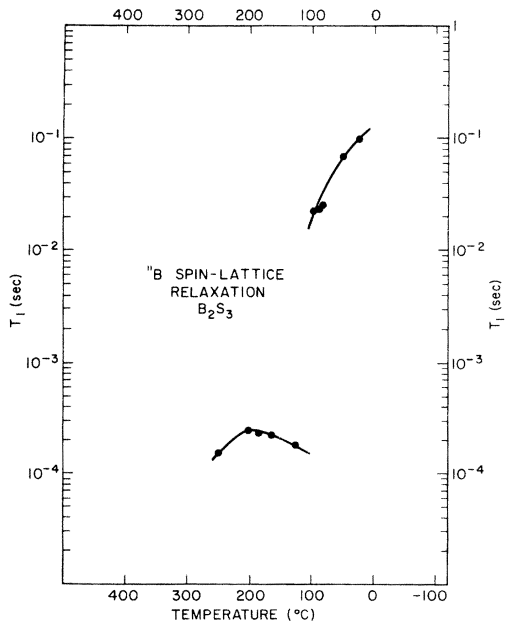

FIG. 7. Temperature variation of the ^{11}B spin-lattice relaxation time in B_2S_3 at 15.450 MHz.

Above 100 °C the symmetric line gradually disappeared, and an extremely narrow line or "spike" grew in its place with increasing temperature. The amplitude of the spike as a function of the parameter $1000/T$ is shown in Fig. 8(a), which is taken from the paper by Hendrickson and Bishop.[17] The data are obtained with a cw spectrometer and phase-sensitive detector system in the absorption-derivative mode using a quite small modulating field ~0.1 G. This procedure emphasizes the narrow component of the line. When this process was investigated with pulsed NMR, the effect was somewhat less dramatic; a more gradual evolution of the wider symmetric line into the spike was indicated.

Hendrickson and Bishop attributed this behavior as indicative of a transition from the solid to the viscous phase; but we have argued that the viscous phase has already been attained at 100 °C. An alternate explanation for this effect can be obtained by assuming that the structural model advocated for B_2O_3, and shown in Fig. 1, is also applicable to B_2S_3. In this model, the viscous phase of B_2S_3 is an amalgam composed of various sized clusters. The large clusters are primarily composed of linked six-membered B_3S_3 rings; the smallest clusters are B_2S_3 molecular units. The B_2S_3 molecular units are more mobile than the larger clusters, and their contribution to the NMR linewidth will motionally narrow to a greater extent. As the temperature is raised, the clusters progessively break down into smaller units, forming more B_2S_3 molecules. The intensity of the spike, shown in Fig. 8(a), is then a measure of the number of B_2S_3 molecular units in the melt.

Two comments are worthy of mention at this

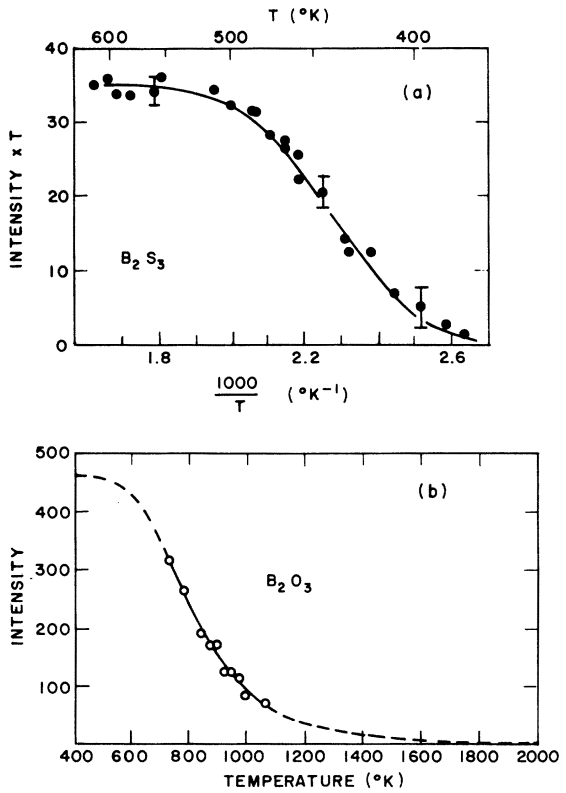

FIG. 8. (a) Temperature dependence of the ^{11}B "spike" intensity in B_2S_3 (from Ref. 17). (b) Temperature dependence of the intensity of the 808-cm^{-1} Raman line in B_2O_3 (from Ref. 4).

point. First, the molecular unit in the vapor phase of boron sulfide has been identified as B_2S_3 by infrared spectroscopy,[16] and has been tentatively assigned a twisted zigzag shape with C_2 symmetry from its isotope shift. Presumably, the same B_2S_3 molecules are present in the high-temperature melt. Secondly, a very minute remnant of the vitreous powder pattern can still be detected in B_2S_3 at temperatures as high as 250 °C. This indicates that break up into smaller clusters is not a homogeneous process, and a very small fraction of the sample consists of units which are large enough to be considered solid fragments, even at high temperatures. This does not occur in B_2O_3, where the glass transition occurs at a much higher temperature.

Figure 8(b) reproduces the temperature dependence of the 808-cm^{-1} Raman-line intensity in B_2O_3.[4] This resonance line is attributed to a breathing mode of the boroxol ring structures in vitreous boron oxide.[13,3] Provided this identification is correct, the intensity of the 808-cm^{-1} line is proportional to the number of six-membered rings in the glass. The decrease in intensity with increasing temperature reflects the gradual conversion of the melt into a molecular fluid. Figures 8(a) and 8(b) are juxtaposed so as to portray the belief that the growth of the NMR spike in B_2S_3 and the decay of the 808-cm^{-1} Raman line in B_2O_3 are caused by identical processes: the progressive fragmentation of the melt into a molecular fluid with increasing temperature. To check this hypothesis, the author suggests to any Raman spectroscopist who has read this far that he investigate the B_2S_3 analog of the 808-cm^{-1} line. Using simple mass scaling, this line can be expected to occur near 570 cm^{-1} in B_2S_3. It is anticipated that the intensity of this Raman line will continuously decrease with increasing temperature above 100 °C and will vanish near 200 °C.

SUMMARY AND ACKNOWLEDGMENTS

We have investigated the ^{11}B NMR line shape and the spin-lattice relaxation of amorphous B_2O_3 and B_2S_3 as a function of temperature in the glass transformation region and beyond. The spin-lattice relaxation has been correlated with the dynamical processes of B_2O_3 glass. A local T_1 minimum which occurs around 50 °C, is attributed to a two-phonon Raman process involving "extra" low-frequency lattice vibrations whose lifetimes are strongly temperature dependent. A second T_1 minimum is predicted to occur at ~1000 °C, and is caused by rapid thermal motions which modulate the nuclear quadrupole interaction. We have utilized existing data on the temperature dependence and distribution of the correlation times in B_2O_3 to explain the spin-lattice relaxation behavior at elevated temperatures. Finally, a structural model of B_2O_3 has been advocated which seems consistent with the available data.

We have proposed that vitreous B_2S_3 has the same basic structure of B_2O_3, and undergoes similar structural changes with increasing temperature. However, data from other experiments, so abundant in B_2O_3, are lacking in B_2S_3, and we have not carried the theoretical analysis as far. Our data indicate that the glass transformation temperature in B_2S_3 occurs near 100 °C (compared to 280 °C in B_2O_3), and that B_2S_3 behaves as a molecular fluid above 200 °C.

The author is grateful to Dr. S. Bishop and Dr. P. Kline for supplying samples of B_2S_3 and B_2O_3. Dr. R. Corsaro is thanked for sharing his extensive reprint collection. The author is also pleased to acknowledge Dr. Henry Resing for numerous useful discussions.

[1]M. Rubinstein and H. A. Resing, Phys. Rev. B 13, 959 (1976); M. Rubinstein, H. A. Resing, T. L. Reinecke, and K. L. Ngai, Phys. Rev. Lett. 34, 1444 (1975).
[2]R. L. Mozzi and B. E. Warren, J. Appl. Crystallogr. 3, 251 (1970).
[3]A. H. Silver and P. J. Bray, J. Phys. Chem. 29, 984 (1958); D. Kline, P. J. Bray, and H. M. Kriz, J. Chem. Phys. 48, 5277 (1968).
[4]T. F. Young and R. P. Westerdahl, ARL 135, OAR, U.S. Air Force, 1961 (unpublished).
[5]J. Goubeau and H. Keller, Z. Anorg. Chem. 272, 303 (1953).
[6]J. Krogh-Moe, Phys. Chem. Glasses 6, 46 (1965).
[7]A. Napolitano, P. B. Macede, and E. G. Hawkins, J. Am. Ceram. Soc. 48, 613 (1965).
[8]J. Boow, Phys. Chem. Glasses 8, 45 (1967).
[9]L. L. Sperry and J. D. Mackenzie, Phys. Chem. Glasses 9, 91 (1968).
[10]J. Tauke, T. A. Litovitz, and P. B. Macedo, J. Am. Ceram. Soc. 51, 158 (1968).
[11]P. B. Macedo, W. Capps, and T. A. Litovitz, J. Chem. Phys. 44, 3357 (1966).
[12]J. Bucaro, H. D. Dardy, and R. D. Corsaro, J. Appl. Phys. 46, 741 (1975).
[13]J. Krogh-Moe, J. Non-Cryst. Solids 1, 269 (1969).
[14]J. D. Mackenzie, J. Phys. Chem. 63, 1875 (1959).
[15]P. L. Hanst, V. H. Early, and W. Klemperer, J. Chem. Phys. 42, 1097 (1965).
[16]F. T. Greene and J. L. Margrave, J. Am. Chem. Soc. 81, 5555 (1959).
[17]J. R. Hendrickson and S. G. Bishop, Solid State Commun. 17, 301 (1975).
[18]H. A. Resing, J. Chem. Phys. 43, 669 (1965).
[19]W. G. Clark, Rev. Sci. Instrum. 35, 316 (1964).
[20]A. Abragam, *The Principles of Nuclear Magnetism* (Clarendon, Oxford, 1961).
[21]The ^{10}B resonance in B_2O_3 is discussed by L. W. Panek, G. E. Jellison, and P. J.Bray, Bull. Am. Phys. Soc. 21, 459 (1976).
[22]H. M. Kriz and P. J. Bray, J. Non-Cryst. Solids 6, 27 (1971).
[23]M. H. Cohen and F. Reif, in *Solid State Physics*, edited by F. Seitz and D. Turnbull (Academic, New York, 1957), Vol. 5.
[24]J. Szeftel and H. Alloul, Phys. Rev. Lett. 34, 657 (1975).
[25]W. A. Phillips, J. Low Temp. Phys. 7, 351 (1972); P. W. Anderson, B. I. Halperin, and C. M. Varma, Philos. Mag. 8, 1 (1972).
[26]T. L. Reinecke and K. L. Ngai, Phys. Rev. B 12, 3476 (1975);
[27]J. Van Kronendonk, Physica (Utr.) 20, 781 (1954).
[28]G. Winterling, Phys. Rev. B 12, 2432 (1975).
[29]N. Bloembergen, E. M. Purcell, and R. V. Pound, Phys. Rev. 73, 679 (1948).
[30]P. S. Hubbard, J. Chem. Phys. 53, 985 (1970).
[31]A. N. Nowick and B. S. Berry, IBM J. Res. Dev. 5, 297 (1961).
[32]C. T. Moynihan, L. P. Boesch, and N. L. Laberge, Phys. Chem. Glasses 14, 122 (1973).
[33]N. H. Ray, Phys. Chem. Glasses 16, 75 (1975).